

Study on Ignition and Combustion Characteristics of Zr-radical or ZrH₂-radical Propellant

Qing Liu¹, Linqun Chen¹, Jianru Wang¹, Baojiang Nan¹, Xue Liu², Yanjun Bai¹, Tuanwei Xu¹

(1. Xi'an Aerospace Solid Propulsion Technology, Xi'an 710025, China ;

2. Hubei Institute of Aerospace Chemotechnology, Xiangyang 441003, China)

Abstract: In order to investigate the influence of Zr(ZrH₂) powder and Zr particle size on the ignition and combustion characteristics of composite propellant, the combustion process of Zr-radical propellant and ZrH₂-radical propellant with the same particle size and Zr-radical propellant with different particle size were studied. The propellant is ignited by a CO₂ laser igniter, and a high-speed camera is used to visualize the propellant combustion process. The spectral thermometer measures the real-time temperature of the combustion. Finally, the microstructure and particle size distribution of the propellant combustion products are analyzed by SEM and particle size analyzer. The experimental results show that as the particle size of the zirconium powder in the propellant increases, the ignition delay time and combustion time increase, and the combustion rate decreases. The combustion time of ZrH₂- radical propellant is significantly lower than that of Zr-radical propellant, and the burning rate is significantly higher than that of Zr-radical propellant. The addition of Zr(ZrH₂) powder to the propellant resulted in more intense side-burning, which indicates that the addition of Zr(ZrH₂) can significantly improve the ignition and combustion performance of the propellant. As the particle size of the zirconium powder increases, the particle size of the product decreases slightly, and the degree of particle agglomeration decreases during combustion. Zr-radical propellant combustion products are cracked spherical bodies and shells, and some slag; while ZrH₂-radical propellant combustion products are mostly in the form of slag, a small part is cracked spherical body and shell Shape.

Key words: Zr-radical propellant; ZrH₂-radical propellant; Particle size; Ignition performance; Combustion performance

1 Introduction

The addition of reactive metal additives to the composite propellant can significantly increase the specific impulse or density specific impulse of the propellant [1]. Zr (ZrH₂) powder is used as a high-density propellant additive, which adding to propellant can increase the density of propellant (2.3~2.5 g/cm³). Further, increasing the speed increment and density specific impulse of the missile [2]. Lempert [3] also pointed out that the best ballistic performance can be obtained when the Zr or ZrH₂ content in the propellant is 37%-46%. Both Byoung [4] and Alekseev [5] found that the effect of large particle Zr powder and small particle Al powder on the burning rate of propellant is about the same. In addition, metal hydride is a good hydrogen storage material with a hydrogen content of 5% to 15% and a volumetric hydrogen density of twice that of liquid hydrogen. Metal hydride is a highly efficient hydrogen release material with a decomposition temperature much lower than burning temperature of propellant [6,7]. Therefore, the addition of metal hydride to the propellant brings new ideas for propellant research [8].

In order to further explore the ignition and combustion properties of Zr-radical and ZrH₂-radical propellants, an experimental study on the combustion process of Zr-radical or ZrH₂-radical propellant

was carried out. Three different formulations of propellant were ignited using a CO₂ laser ignition, while the entire combustion process was recorded using a high speed camera, and the real-time temperature of the combustion was measured by spectral thermometer. In addition, the particle size distribution and microscopic morphology of the combustion products were analyzed by means of a laser particle size analyzer and SEM. A preliminary study on the application of Zr(ZrH₂) in propellants was conducted.

2 Experimental Section

In the experiment, a square piece of 10mm × 10mm × 3mm (shown in Fig. 1) was adhered on the test bench in the combustion chamber, and the position of the laser light was used to ensure that the laser beam was aligned with the center of the propellant block. Turn on the spectral thermometer and start recording the temperature data. Finally, click the ignition button and trigger the high speed camera to start recording the combustion process. Since the shooting of the high-speed camera is triggered synchronously with the laser emitted by the laser, a photo of the flame that maintains the self-sustaining combustion as shown in fig. 2, which the time corresponding to is defined as the ignition delay time of the propellant-- t_d . Similarly, the time during which the flame maintains self-sustaining combustion until the combustion is extinguished is defined as the burning time of the propellant -- t_c . In order to investigate the effects of Zr-radical and ZrH₂-radical propellant ignition combustion performance and the influence of Zr powder particle size on the ignition and combustion performance of propellant, the experimental study on the combustion process was carried out for the three different formulation propellants in Table 1.

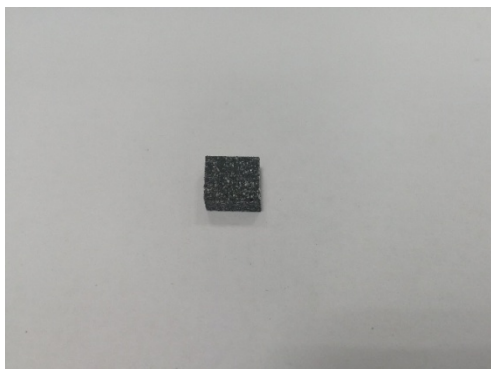


Fig. 1 10mm × 10mm × 3mm propellant block
physical picture

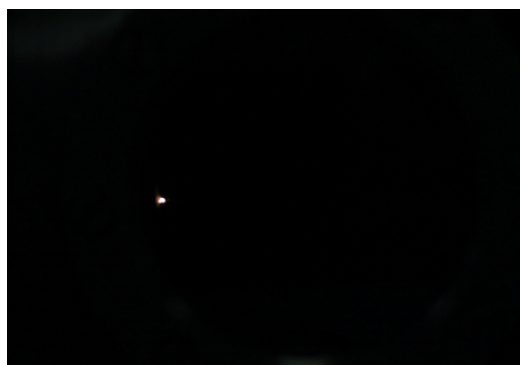


Fig. 2 ignition delay time flame

Table 1 Experimental propellant formula

Propellants	HTPB (%)	AP (%)	30μmZr powder (%)	30μmZrH ₂ powder (%)	15μmZr powder (%)
P1	12	70	0	0	18
P2	12	70	18	0	0
P3	12	70	0	18	0

3 Results and discussion

3.1 Analysis of ignition and combustion characteristics of propellant

In order to investigate the effect of zirconium powder particle size and propellant additive (Zr or ZrH₂) on the ignition and combustion characteristics of propellant, this study designed the ignition experiment of three working conditions of C1, C2 and C3. The laser ignition power is 15 W in the experiment. The propellants P1, P2 and P3 were ignited at a pressure of 1 atm. By conducting these three propellant ignition experiments, the ignition delay time t_d , the combustion time t_c , and the combustion temperature T are obtained as shown in Table 2. As can be seen from Table 2, the ignition delay time of the propellant P1 is the shortest, which is 118 ms, and the ignition delay time of P2 is the longest, which is 136 ms, and the ignition delay time of P3 is close to P2, which is 133 ms. The three propellant blocks with a thickness of 3mm, the P2 propellant has the longest burning time of 3056ms, the P3 propellant has the shortest burning time of 2239ms, and the P1 propellant burning time is 2604ms. The order of burning rate of the three propellants is: P3>P1>P2. It can be seen that as the particle size of the Zr powder in the propellant increases, the ignition delay time increases, the burning time increases, and the burning rate decreases. The smaller the zirconium powder particles, the easier it is to ignite and the faster the burning rate. Therefore, the addition of small particle size Zr powder to the propellant can shorten the ignition delay time and burning time of the propellant and increase the propellant burning rate. In addition, Zr powder and ZrH₂ powder of the same particle size are added to the propellant. The ignition delay time of the two is very close. The ignition delay time of Zr propellant is slightly larger than that of ZrH₂-radical propellant, but the combustion time of ZrH₂-radical propellant is significantly lower than that of Zr-radical propellant. The ZrH₂-radical propellant has a significantly higher burning rate than the Zr-radical propellant. The reason why the burning rate of ZrH₂-radical propellant is higher than that of Zr-radical propellant is that the NO gas generated by AP(NH₄ClO₄) decomposition will adhere to ZrH₂, which promotes the decomposition of AP to produce NO. With the rate of NO production increasing, the rate of reaction of NO with Zr (ZrH₂ decomposes to produce Zr and H₂) increases. On the other hand, the generation of H₂ will slightly increase the combustion chamber pressure and further increase the combustion rate^[9].

The theoretical combustion temperature values of propellants in Table 2 are calculated using the CEA thermodynamic calculation software developed by NASA. By comparing the theoretical temperature value with the measured temperature value, it is found that the difference between the two is no more than 250K, and the experimental value is about 91.59%~94.25% of the theoretical value.

Table 2 Comparison of ignition and combustion characteristics data of working conditions C1~C3

Conditions	Propellants	t_d (ms)	t_c (ms)	T (K)	
				measured values	theoretical value
C1	P1	118	2604	2659	2903
C2	P2	136	3056	2736	2903
C3	P3	133	2239	2570	2791

3.2 Visualization analysis of propellant combustion process

The evolution process of the three propellant combustion flames is shown in Fig.3 to Fig.5. This

experiment uses a high speed camera to visualize the combustion process. Sampling frequency of the camera is 1000Hz. Fig. 3 shows the evolution of the combustion flame of P1 propellant at 1 atm over time. As can be seen from Fig. 3, as time goes by, the flame changes from short to long, from fine to thick, from dark to bright. The inner flame is white, and the outer flame is pale yellow. It can be seen that at the 846ms, there is more severely side-burning on the side surface, and the flame evolves into a "7" shaped flame. When side-burning also occurs on the upper side at around 1258ms, the flame becomes "T" shaped. Finally, as time passed, the flame slowly becomes shorter and darker until it went out.

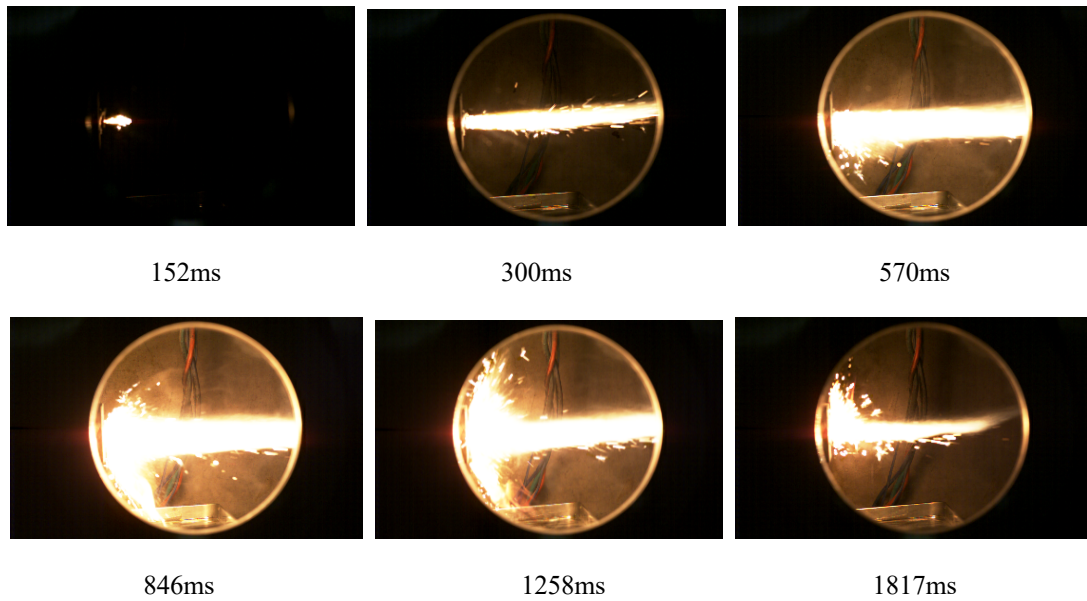


Fig. 3 Evolution of P1 propellant combustion flame

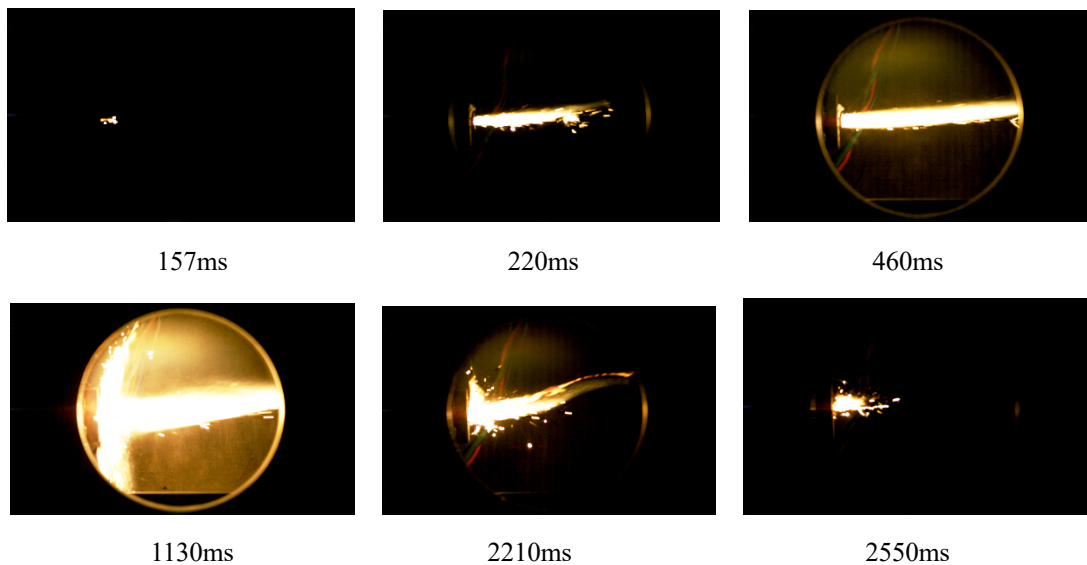


Fig.4 Evolution of P2 propellant combustion flame

As can be seen from Fig. 4, as time goes by, the P2 propellant starts to ignite, the flame gradually becomes longer and thicker, and the brightness is gradually increased. The flame is straight in the

initial stage of combustion, but gradually begins to have more serious side burning. At the 1130ms, the sides surfaces began to burn, thus forming a "T" shaped flame. Before that, the side-burning flame and the front-burning flame have a small angle, forming a "trident" shaped flame. The "trident" shaped flame evolved into a "T" shaped flame over time. Finally, the flame size gradually becomes smaller, the brightness is gradually lowered, and it is slowly extinguished. It can be seen from the shape of the flame that the side-burning level of the P2 propellant and the P1 propellant is very close. It is speculated that the possible reason for the formation of side-burning is that after the addition of Zr powder, the ignition delay time of the propellant is reduced, and the heat is heated to heat the side of the propellant faster. Since the Zr powder is more flammable, the temperature being relatively low and the sides are uncoated and extinguished, thus causing side-burning. Therefore, it can be considered that the ignition performance and the combustion characteristics of the propellant are improved after the addition of the zirconium powder.

The evolution of the combustion flame of P3 propellant at 1 atm is shown in Fig.5. As can be seen from Fig. 5, as time passes, the flame changes from short to long, from fine to thick, from dark to bright. The inner flame is white, and the outer flame is pale yellow. It can be seen that there is a more severe side-burning around 900ms, and the flame evolves into a "T" shaped flame. This is roughly the same as the evolution of the P2 propellant flame. It is difficult to judge from the flame size and shape that the side-burning of the two propellants is more serious. For this purpose, the duration of the two propellant side-burning and the entire burning time are calculated. The ratio is used as the basis for judging the degree of side-burning. It is found by calculation that the ratio of P2 propellant is 0.59, and that of P3 propellant is 0.62, which is slightly higher than that of P2 propellant. Therefore, it can be considered that the side-burning of P3 propellant is slightly more serious than that of P2 propellant. That is to say, the ignition and combustion performance of P3 propellant is slightly better than P2 propellant.

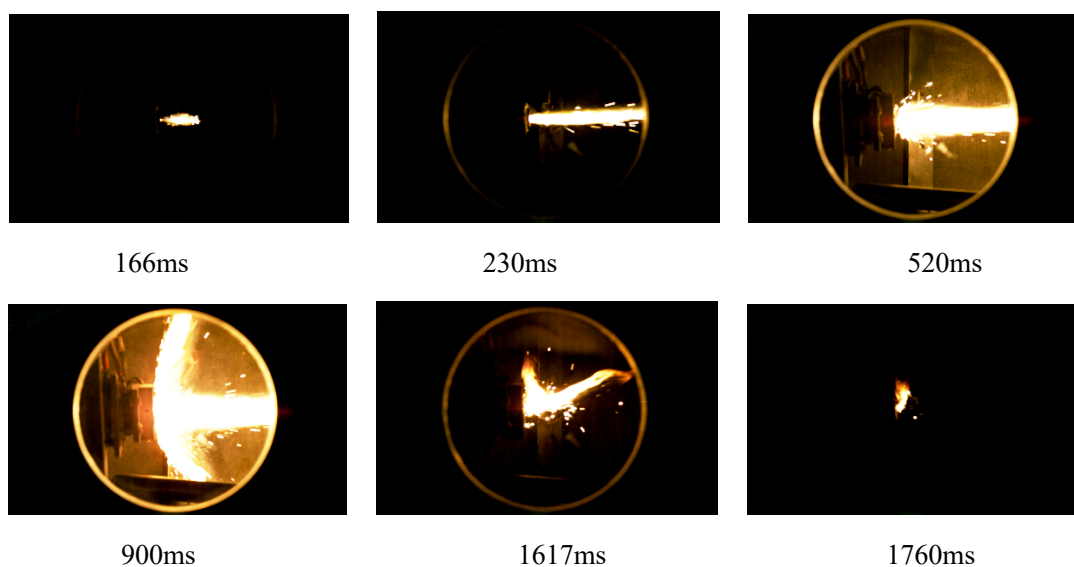


Fig.5 Evolution of P3 propellant combustion flame

3.3 Propellant combustion product particle size analysis

The particle size distribution of the three propellant combustion products is shown in Fig.6 to Fig.8. It

can be seen from Fig. 6 that the distribution of combustion products of propellant P1 ranges from 7 μm to 120 μm, the particles are mainly distributed between 35 μm and 75 μm, accounting for 51%. The particles below 10 μm only account for 3%, and the particles above 100 μm only account for 2.1%. The volume average diameter $D(4,3)$ of the P1 propellant combustion product particle diameter is 48.44 μm, and the median diameter D_{50} is 45.26 μm. It can be seen from Fig. 7 that the particle size of the P2 propellant combustion product is mainly distributed between 4 μm and 120 μm, and more than 70% of the particle size distribution is within 25 μm to 65 μm. The volume average diameter $D(4,3)$ of the particle size of the propellant P2 combustion product is 42.74 μm, and the median diameter D_{50} is 39.77 μm. It can be seen from Fig. 8 that the distribution of the combustion products of the propellant P3 ranges from 1 μm to 160 μm, the particles are mainly distributed between 40 μm and 85 μm, accounting for about 35%. The particles below 5 μm are about 4%, and the particles above 100 μm are about 6.5%. The volume average diameter $D(4,3)$ of the particle size of the propellant P3 combustion product is 44.49 μm, and the median diameter D_{50} is 39.41 μm.

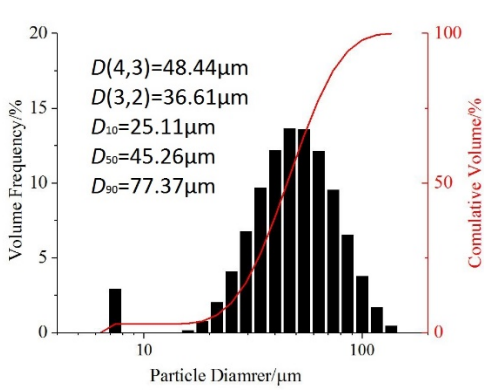


Fig.6 Particle size distribution of P1 propellant combustion products

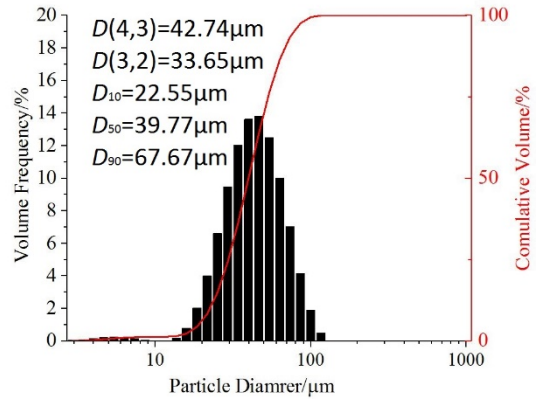


Fig.7 Particle size distribution of P2 propellant combustion products

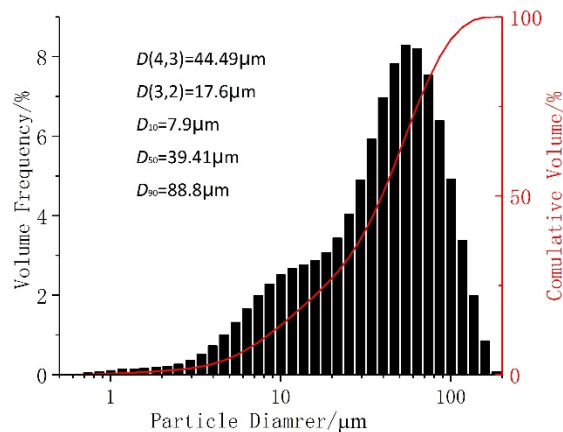


Fig.8 Particle size distribution of P3 propellant combustion products

It can be seen from the above analysis that the particle size of the P1 propellant combustion product is relatively large, and the particle size of the P2 and P3 propellant combustion products is relatively smallest. Comparing the particle size of the P1 propellant and P2 propellant combustion products, it is found that the particle size of the propellant P1 combustion product is slightly higher

than that of the P2 propellant, and the particle size of the propellant is relatively close. The reason for this phenomenon is that the size of the zirconium powder particles is small, and the phenomenon of particle agglomeration is more serious during combustion. Comparing the particle size of the combustion products of P2 and P3, the particle size of the combustion product of propellant is close to that of P2 propellant, but the particle distribution of propellant P3 product is more dispersed, while the particle size of P2 product is more concentrated.

3.4 Analysis of Microscopic Morphology of Propellant Combustion Products

The microscopic morphology of the propellant P1 combustion product under SEM is shown in Fig. 9. The results of EDS analysis of the combustion products are shown in Fig. 10 and Table 3. It can be seen from Fig. 9(a) that the P1 combustion products are mainly cracked spherical bodies and some slags, in addition to some spherical bodies and shells. The center position of Fig. 9(b) is a gray shell, and the upper side is a spherical body attached to some white particles, and a cracked spherical body on the below side. Fig. 9(c) shows a spherical body with many cracks on the surface, and some broken spherical bodies. The EDS analysis of the white particles and the gray shell on the surface of the spherical body in Fig. 9(b) shows that the atomic ratio of Zr to O in the particles is 3:2, and the atomic ratio of the gray shell is close to 3:2. The ratio of Zr element to O element of ZrO₂ is 1:2. So it can be seen that both ZrO₂ and metal Zr exist in both places, and the metal Zr content of the gray shell is slightly lower. The EDS of the cracked spherical body in Fig. 9(c) shows that the surface Zr and O atomic ratio is also 3:2, that is, the surface thereof is also a mixture of ZrO₂ and Zr.

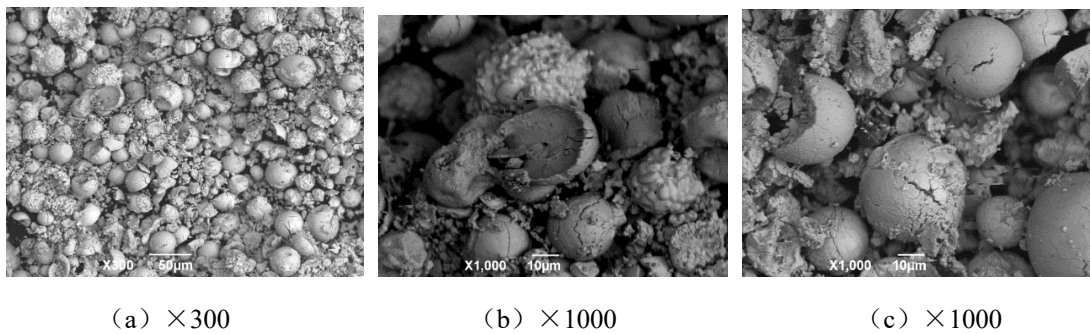
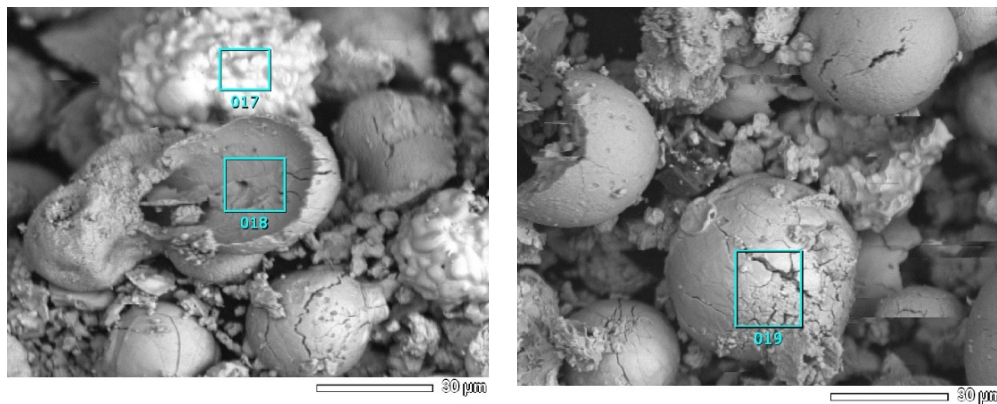
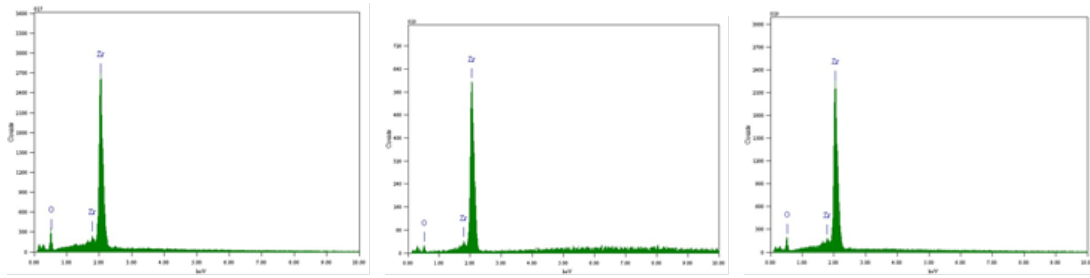


Fig.9 Microstructure of P1 propellant combustion products



(a) sampling points



(b) point 17

(c) point 18

(d) point 19

Fig. 10 EDS analysis results of P1 propellant combustion products

Table 3 Proportion of atomic atoms at each sampling point of propellant P1 combustion products

Element	Atom/%		
	point 17	point 18	point 19
O K	40.90	43.49	39.82
Zr L	59.10	56.51	60.18

The microscopic morphology of the propellant P2 combustion product under SEM is shown in Fig. 11, and the EDS analysis results of the P2 combustion product are shown in Fig. 12 and Table 4. It can be seen from Fig. 11(a) that there are mainly three structures in the P2 combustion product, ones are some relatively regular spheres and ellipsoids, but most of the surfaces have cracks or white particles attached to; the other are some shell and Broken hemisphere; the last are some irregularly shaped slag. As can be seen from Fig. 11(b), these spherical bodies have a diameter of about 30 μm , a large number of cracks on the surface, or a rough surface, and white granular particles adhered thereto. It can be seen from Fig. 12 and Table 4 that the surface of the cracked sphere is mainly O and Zr elements, and the ratio of the two is about 1:1, so it can be inferred that the surface has not only ZrO_2 but also metal Zr. The elements of the white particles attached to the surface mainly have O and Zr, and the atomic ratios of the two element are 36.27% and 63.73%, respectively, and there are both ZrO_2 and metal Zr. Fig. 11 (c) and (d) are enlarged views of the broken shell and the hemisphere, respectively, and the surface thereof is rough. By analyzing the microscopic morphology and EDS results of the P2 and P1 propellant combustion products, it is known that the combustion products of the Zr-radical propellant are mainly broken, cracked spherical bodies, and some irregular slag. There are both ZrO_2 and Zr in the combustion products, and the ratio of the two is close to 1:2.

Table 4 Proportion of atomic atoms at each sampling point of P2 propellant

Element	Atom (%)	
	point 12	point 13
O K	48.11	36.27
Zr L	51.89	63.73

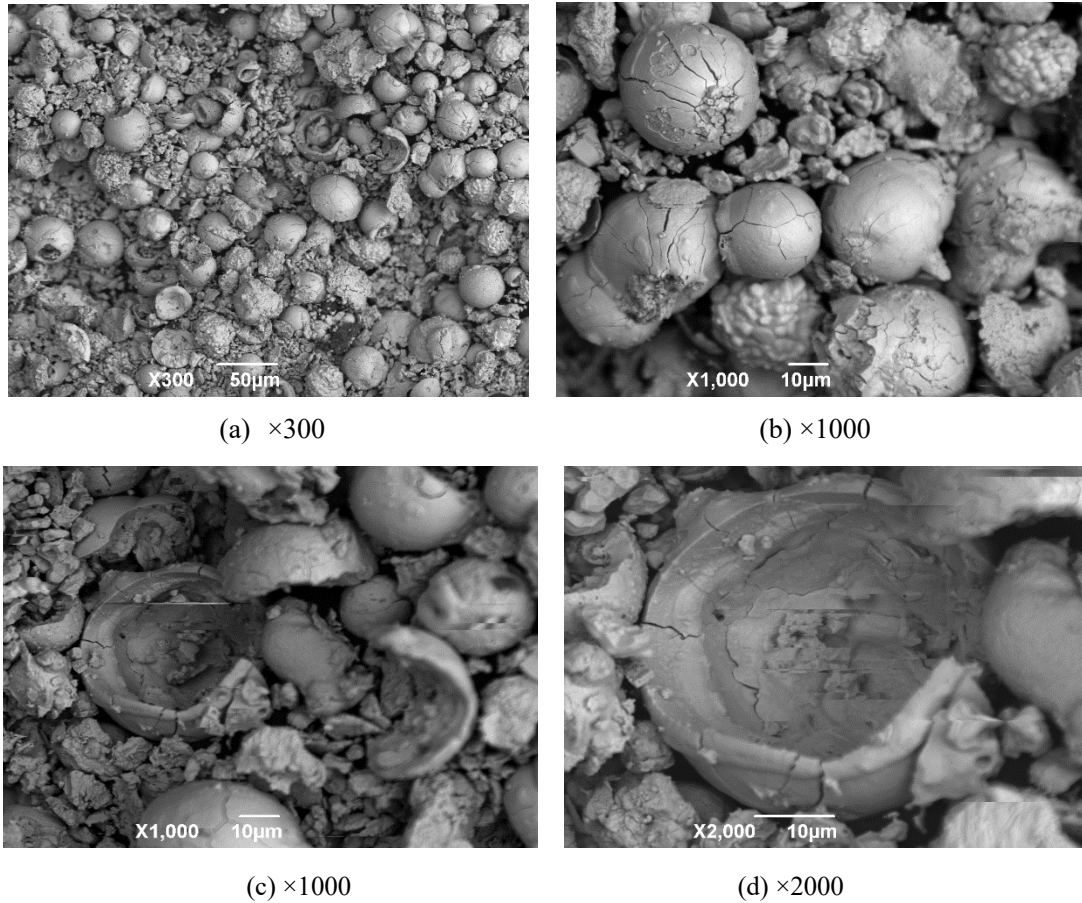


Fig. 11 Microstructure of P2 propellant combustion products

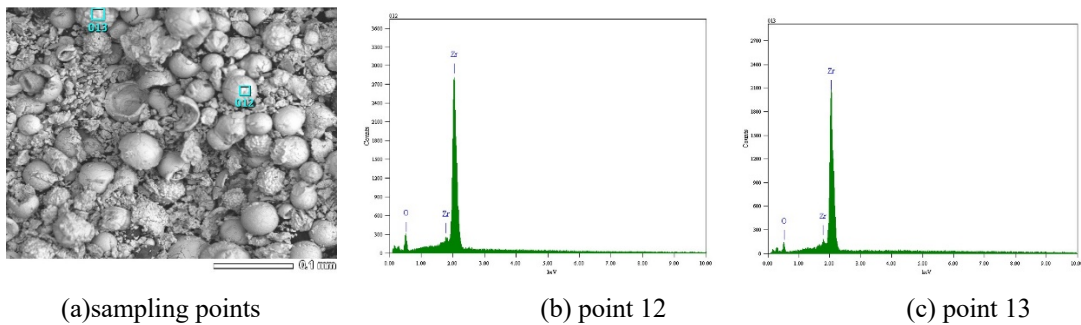


Fig.12 EDS analysis results of P4 propellant combustion products

The microscopic morphology of the propellant P3 combustion product under SEM is shown in Fig. 13. The EDS analysis results of the P3 propellant combustion product are shown in Fig. 14 and Table 5. It can be seen from Fig. 13(a) that most of the combustion products of the P3 propellant are irregular slag and large-sized lumps piled up by small particles, and only a small part is a relatively regular spheroid, which surface is rough and is attached to some slag. The center position of Fig. 13(b) is a spherical body with a smooth surface with a diameter of about 23 µm. The surface EDS analysis shows that there are mainly Zr and O elements on the surface, and the atomic ratio of the two is about 3:2. From this, it is understood that the surface components are ZrO₂ and metal Zr. The EDS analysis results of the slag in the combustion products and the larger size block is in a similarity to the

spheroid, and the ratio of the Zr atom to the O atom is also about 3:2. Comparing with the P2 propellant combustion products, it can be seen that the P2 propellant combustion products are relatively regular, mostly spherical, and slightly larger in size than the P3 propellant combustion products.

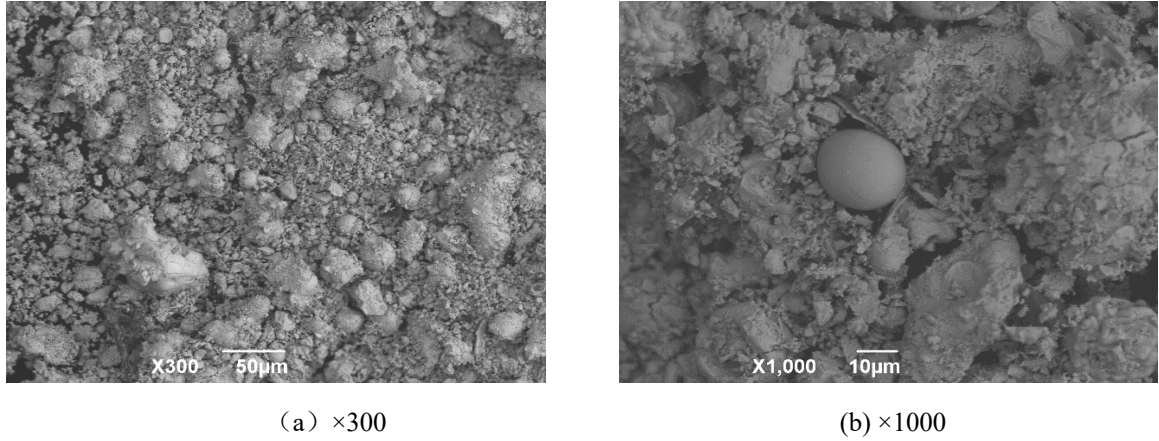


Fig.13 Microstructure of P3 propellant combustion products

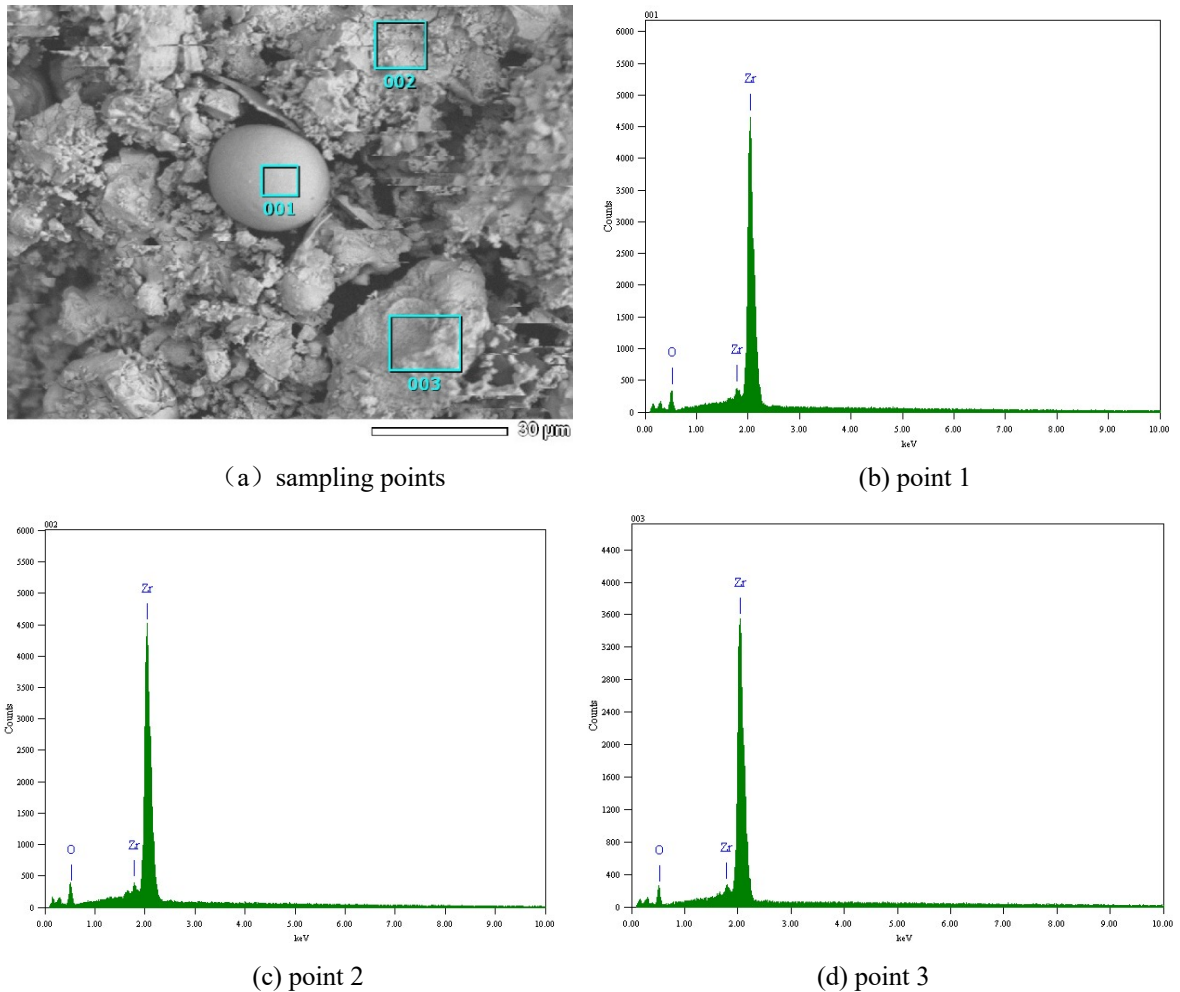


Fig.14 EDS analysis results of P3 propellant combustion products

Table 5 Proportion of atomic atoms at each sampling point of P3 propellant combustion products

Element	Atom (%)		
	point 1	point 2	point 3
O K	40.90	43.49	39.82
Zr L	59.10	56.51	60.18

4 Conclusion

(1) The ignition delay times of the three propellants are 118 ms, 136 ms, and 133 ms, respectively; the combustion times are 2603 ms, 3056 ms, and 2239 ms. Therefore, as the particle size of the zirconium powder in the propellant increases, both the ignition delay time and the combustion time increase, and the burning rate decreases. The ignition delay time of Zr-radical propellant and ZrH₂-radical propellant is very close, but the combustion time of ZrH₂-radical propellant is significantly lower than that of Zr-radical propellant, and the burning rate is significantly higher than that of Zr-radical propellant.

(2) Zr(ZrH₂) powder is added to the propellant, and the propellant shows more severe side-burning, which indicates that the addition of Zr(ZrH₂) can significantly improve the ignition and combustion performance of the propellant.

(3) The volume average diameter $D(4,3)$ of the P1, P2 and P3 propellant combustion product particle diameters are 48.44 μm , 42.74 μm and 44.49 μm , respectively; the median diameter D_{50} are 45.26 μm , 39.77 μm and 39.41 μm , respectively. As the particle size of the zirconium powder increases, the particle size of the product decreases slightly, and the degree of particle agglomeration decreases during combustion. The Zr-radical propellant and the ZrH₂-radical propellant combustion products are very close, but the Zr-radical propellant product particle size distribution is relatively more concentrated.

(4) Zr-radical propellant combustion products are cracked spherical bodies and shells, and some slag; while ZrH₂-radical propellant combustion products are mostly in the form of slag, a small part is cracked ball Shape and shell.

References:

- [1] Pang, Wei - Qiang, Fan, Xue - Zhong, Zhao, Feng - Qi, et al. Effects of Different Nano - Metric Particles on the Properties of Composite Solid Propellants[J]. Propellants Explosives Pyrotechnics, 2014, 39(3):329-336.
- [2] Lempert D B, Brambilla M, Deluca L T. Ballistic effectiveness of Zr-containing composite solid propellants as a function of binder nature and mass fraction[J]. Eucass Proceedings, 2013, 4:15-32.
- [3] Lempert D B, Nechiporenko G N, Manelis G B. Energetic capabilities of high-density composite solid propellants containing zirconium or its hydride[J]. Combustion Explosion & Shock Waves, 2011, 47(1):45-54.

- [4] Min B S, Hyun H S. Study on Combustion Characteristics and Performance of HTPB/AP Propellants Containing Zirconium[J]. Journal of Propulsion & Power, 2015, 28(1):211-213.
- [5] Alekseev A P, Lempert D B, Nemtsev G G, et al. Combustion of zirconium-containing model compositions of solid propellant[J]. Russian Journal of Physical Chemistry B, 2012, 5(6):997-999.
- [6] Bazyn T, Eyer R, Krier H, et al. Dehydrogenation and Burning of Aluminum Hydride at Elevated Pressures [C]//Aiaa Aerospace Sciences Meeting & Exhibit. 2013.
- [7] Grochala W, Edwards P P. Thermal decomposition of the non-interstitial hydrides for the storage and production of hydrogen.[J]. Chemical Reviews, 2004, 104(3):1283-1316.
- [8] A.E.D.M. van der Heijden, Leeuwenburgh A B. HNF/HTPB propellants: Influence of HNF particle size on ballistic properties [J]. Combustion & Flame, 2009, 156(7):1359-1364.
- [9] Yanjing-Yang, Fengqi-Zhao, Zhifeng-Yuan, et al. On the combustion mechanisms of ZrH₂ in double-base propellant[J]. Physical Chemistry Chemical Physics, 2017, 48(19):32597-32604.